

De Haas-van Alphen Effect in Tin and Tin-Antimony Alloys*†

G. T. CROFT,‡ W. F. LOVE, AND F. C. NIX

Randal Morgan Laboratory of Physics, University of Pennsylvania, Philadelphia, Pennsylvania

(Received May 24, 1954)

The de Haas-van Alphen effect has been studied in a series of dilute alloys of tin with antimony at field strengths below 10 000 gauss. Over the range of compositions studied (0–0.23 atomic percent Sb) there was no observable change in the parameters characterizing the de Haas-van Alphen effect other than the collision broadening parameter X , which increased uniformly with concentration of antimony. The temperature dependence of the amplitude of the susceptibility oscillations agrees with the theoretical predictions, but there is evidence that the field dependence does not. An angular dependence of X was observed and interpreted in terms of the lattice geometry. The room temperature magnetic anisotropy was also measured and found to increase by approximately 25 percent for an antimony concentration of 0.23 atomic percent.

I. INTRODUCTION

SINCE the original discovery by de Haas and van Alphen¹ of the oscillating behavior of the magnetic moment of a bismuth crystal as a function of the magnetic field strength, this effect has been discovered and studied in a number of different metals. The object of this investigation was to determine the various effects on this phenomenon due to alloying. The system tin-antimony was chosen as the most suitable for a study of this kind since its tin-rich alloys are substitutional solid solutions possessing a sufficient range of solid solubility to determine these effects, and because its composition and thermal equilibrium state can be easily controlled. In addition, it allows the variation of the concentration of valence electrons, an important parameter in the theory of the de Haas-van Alphen effect. The effect was first observed in tin by Shoenberg² and has also been reported by Croft, Love, and Nix,³ Berlincourt,⁴ and Verkin, Lazarev, and Rudenko.⁵

The theory as developed by Landau,⁶ Peierls,⁷ Blackman,⁸ Dingle,⁹ and Robinson¹⁰ gives for the difference of susceptibilities of the conduction electrons (considered free, but with tensor effective mass) along two crystallographic directions the following formula:

$$\chi_3 - \chi_1 = \Delta\chi = \frac{e^2(m_1 - m_3)}{12\pi^2 c^2 \hbar m_1} \left(\frac{2\zeta}{m_3}\right)^{\frac{1}{2}} \left\{ 1 - 3\pi\zeta^{\frac{1}{2}} kT(\beta H)^{-\frac{1}{2}} \right. \\ \left. \times \sum_{n=1}^{\infty} \frac{(-1)^n \sin(n\pi\zeta/\beta H - \frac{1}{4}\pi)}{n^{\frac{1}{2}} \exp(-n\pi^2 kX/\beta H) \sinh(\pi^2 kT/\beta H)} \right\}, \quad (1)$$

* Based on the Ph.D. dissertation of G. T. Croft at the University of Pennsylvania.

† Supported by the U. S. Atomic Energy Commission.

‡ Now at the Edison Research Laboratory, of Thomas A. Edison, Inc., West Orange, New Jersey.

¹ W. J. de Haas and P. M. van Alphen, Leiden Comm. No. 212a (1930).

² D. Shoenberg, Nature 164, 225 (1939).

³ Croft, Love, and Nix, Phys. Rev. 86, 650 (1952).

⁴ T. G. Berlincourt, Phys. Rev. 88, 242 (1952).

⁵ Verkin, Lazarev, and Rudenko, J. Exptl. Theoret. Phys. (U.S.S.R.) 20, 995 (1950).

⁶ L. D. Landau, see Appendix to D. Shoenberg, Proc. Roy. Soc. (London) A170, 341 (1939).

⁷ R. Peierls, Z. Physik 80, 763 (1933).

⁸ M. Blackman, Proc. Roy. Soc. (London) A166, 1 (1938).

⁹ R. B. Dingle, Proc. Roy. Soc. (London) A211, 517 (1952).

¹⁰ J. E. Robinson, thesis, Yale University, 1950 (unpublished).

which can be approximated by

$$\Delta\chi = \frac{e^2(m_1 - m_3)}{12\pi^2 c^2 \hbar m_1} \left(\frac{2\zeta}{m_3}\right)^{\frac{1}{2}} \left\{ 1 - 6\pi\zeta^{\frac{1}{2}} kT(\beta H)^{-\frac{1}{2}} \right. \\ \left. \times \exp\left(-\frac{\pi^2 k(T+X)}{\beta H}\right) \sin\left(\frac{\pi\zeta}{\beta H} - \frac{\pi}{4}\right) \right\} \quad (2)$$

if $\pi^2 kT/\beta H \gg 1$. The symbols are defined as follows:

χ_1, χ_3 = magnetic susceptibilities along the 1 and 3 axes, respectively;

ζ = effective Fermi level of the electrons responsible for the effect;

m_1, m_3 = effective mass parameters of the relevant electrons along the 1 and 3 axes, respectively;

$X = \hbar/\pi k\tau$ = collision broadening parameter, where τ = mean free time between collisions for the relevant electrons;

ϕ = angle between the 3 axis of the crystal and the magnetic field H , and

$$(2\beta)^2 = \frac{e^2 \hbar^2}{c^2} \left(\frac{\cos^2 \phi}{m_1^2} + \frac{\sin^2 \phi}{m_3^2} \right). \quad (3)$$

The other symbols have their usual meaning.

In deriving this formula, it is assumed that the electrons responsible for the effect occupy electronic states in \mathbf{k} space on the surface of an ellipsoid of revolution and that the electrons are in an infinitely large volume.

By adjusting the parameters m_1, m_3, ζ , and X , the experimental data can be fitted to the theoretical expression. In order to obtain a fit for tin, values of the following order of magnitude must be assigned to these parameters:

$$\zeta = 0.20 \text{ ev}, \quad X = 0.1^\circ \text{K}, \quad m_1 \cong 0.1m_0, \quad m_3 \cong 1.0m_0,$$

where m_0 is equal to the free electron mass. Using these values, the total number of electrons responsible for the effect is approximately 10^{-3} electron per atom. On the basis of these results, it seems reasonable to attribute the effect to those electrons which occupy states

in \mathbf{k} space just under or overlapping a Brillouin zone boundary.

The expected effects of adding antimony to tin should be to increase the electron concentration and the amount of impurity scattering. If the effect is due to holes, an increase in electron concentration should decrease ζ , and if the effect is attributable to electrons, ζ should increase. Depending on the direction in which ζ tends, it should be possible to determine whether electrons or holes are responsible for the effect. In-

creasing the number of antimony atoms in the lattice should cause a decrease in the mean free time τ , or an increase in the collision broadening parameter X .

II. THE SAMPLES

The alloys used in these experiments were prepared from spectrographically pure components. An analysis of the tin (supplied by A. D. MacKay, Inc.) and antimony (Johnson Matthey No. 660, laboratory No. 4470) gave the following impurities:

For Sn: Pb—0.0012 percent,	S —0.00003 percent,	Bi—0.00012 percent,
Fe—0.00027 percent,	Sb—0.001 percent,	As—0.0002 percent,
Cu—0.0002 percent,	Sn—99.997 percent,	
For Sb: Ni—0.0087 percent,	Fe—0.0013 percent,	Co—Trace,
Other impurities—0.064 percent,	Sb—99.9 percent.	

The compositions of the alloys used in these experiments and other relevant data are given in Table I.

The alloys were made by melting Sb and Sn in proper proportions *in vacuo* in a sealed Pyrex tube. To insure a homogeneous alloy, the melt was vigorously shaken before it was allowed to solidify.

Spherical $\frac{5}{16}$ -in. diameter single crystals were then grown in very high purity graphite molds. These crystals were then annealed in evacuated Pyrex tubes. For annealing times and temperature, as well as the general condition of the samples, refer to Table I. Great care was taken in handling the crystals to avoid straining them in any way.

Each sample was checked for ferromagnetic impurities by the method of the Honda plot.¹¹ Only samples with no detectable trace of ferromagnetic impurity were used in these experiments.

After etching in concentrated HCl, the crystals were oriented by observing the reflections from the etch planes using standard optical techniques. They were then carefully mounted on the suspension of the torsion apparatus with a binary axis directed along the axis of the suspension.

TABLE I. Composition, heat treatment, and condition of samples studied.

Nominal conc. at. % Sb	Spec. analysis at. % Sb	Wt. of sample grams	Annealing ^a time (days)	Condition of sample
0.0	0.002	1.936	1	Single crystal
0.02	0.026	1.802	3	Single crystal
0.05	0.043	1.906	30	Small surface crystallite 1% of total surface
0.10	0.12	1.840	2	Small surface crystallite 1% of total surface
0.20	0.23	1.964	25	Single crystal

^a Annealing temperature of all samples is 145°C.

¹¹ L. F. Bates, *Modern Magnetism* (Cambridge University Press, Cambridge, 1951), third edition, p. 133.

III. THE INSTRUMENTATION

If a spherical single crystal of tin is suspended in a homogeneous magnetic field H such that a binary axis is along the suspension, the torque acting on the sample about the axis of suspension is

$$C = (\chi_3 - \chi_1) H^2 \sin\phi \cos\phi, \quad (4)$$

where χ_3 and χ_1 refer to the susceptibility along the tetragonal and binary axes, respectively, and ϕ is the angle between the tetragonal axis and the magnetic field vector.

In these experiments, the torque C was measured at different temperatures as a function of H , and at vari-

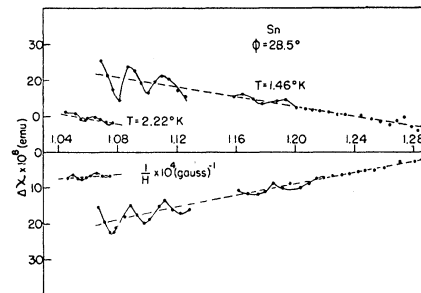


FIG. 1. Typical results for the de Haas-van Alphen effect in tin.

ous angles. From these data, $\Delta\chi$ was easily calculated using the formula given above.

In the case of tin, this low-temperature measurement of the torque by measuring the angular deflection of a torsion suspension presents difficulties not encountered at room temperature. At low temperatures, the conductivity of tin is considerably higher than at room temperature. As a result of this high conductivity, eddy currents induced by the motion of the sample in the field create such strong damping that excessively long times to reach equilibrium deflections are required for a sensitive suspension, and the problem of taking detailed data becomes extremely tedious and time-con-

suming. Another difficulty arises from small changes in orientation of the crystal relative to the magnetic field vector brought about by rotation of the crystal under the influence of the torque due to the de Haas-van Alphen effect alone. Since the period and amplitude of the susceptibility are very sensitive to changes in orientation, rotation of this sort is objectionable and may lead to erroneous results.

Both of the above effects may be eliminated by using a sufficiently stiff suspension in the torsion apparatus. This has been accomplished by an especially designed recording electronic torque meter,¹² which works as follows: The sample was suspended from the suspension coil of a standard wall type galvanometer. By sending a current through this coil, the torque due to the magnetic field could be counterbalanced. This current provided a measure of the torque. A beam of light was reflected from the mirror of the suspension to a split-photocell, high-gain dc amplifier whose output was fed back degeneratively to the suspension coil. The feedback current was made of the order of milliamperes by properly shunting the suspension coil and recorded on a recording milliammeter. This arrangement is tantamount to a very stiff suspension. The maximum angular displacement of the sample was estimated to be 10^{-8}

TABLE II. Comparison of data on Sn.

	ζ in eV	$2\beta \times 10^{20}$ (erg) ⁻¹	ϕ	m_1	m_2
Berlincourt	0.204	16.1	29°	$0.10m_0$...
Croft <i>et al.</i>	0.193	16.2	28.5°	$0.10m_0$	$2.0m_0$
Shoenberg	0.19	...		$0.10m_0$	$2.0m_0$

radian in these measurements. The current through the magnet was provided by motor driven powerstats which supplied voltage to a three-phase full wave rectifier circuit, and was recorded by a recording potentiometer. Effectively, the two quantities, torque and magnetic field, were then recorded simultaneously as the field was slowly decreased, the rate of change of field strength being kept so small that no torques due to eddy currents were produced. This was checked by suddenly stopping the reduction of the field and observing no change in the torque measured.

The electromagnet used had 4-in. diameter pole faces with a 2-in. gap, and was capable of producing magnetic fields up to 9500 gauss. It was calibrated using nuclear resonance techniques. No detectable inhomogeneity in the field was present in the region occupied by the sample.

IV. THE EXPERIMENTAL RESULTS

1. Pure Tin

Qualitatively, the results for pure Sn are similar to those obtained by Shoenberg¹³ and Berlincourt.⁴ Even

¹² Rev. Sci. Instr. (to be published).

¹³ D. Shoenberg, Proc. Roy. Soc. (London) A245, 1 (1952).

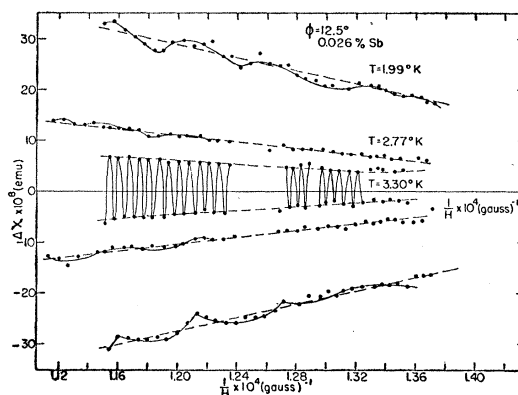


FIG. 2. The de Haas-van Alphen effect in Sn+0.026 atomic percent Sb at $\phi = 12.5^\circ$.

though the range of field strengths is below that of previous workers, the phenomenon of "beats" is still observed. An example of the results for pure Sn is shown in Fig. 1.

Quantitative comparison of the pure Sn data with the results of Shoenberg and Berlincourt (where comparison was possible) is shown in Table II. As far as parameters associated with the period and temperature dependence of the oscillations are concerned, the agreement is good. Comparison of absolute values of $\chi_3 - \chi_1$ was not made

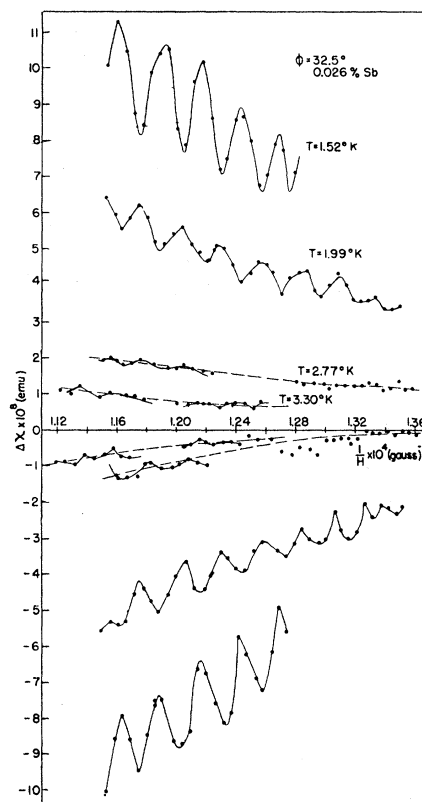


FIG. 3. The de Haas-van Alphen effect in Sn+0.026 atomic percent Sb at $\phi = 32.5^\circ$.

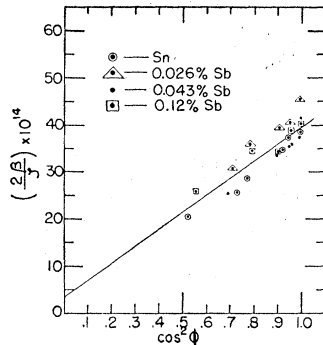


FIG. 4. Plot of $(2\beta/\zeta)^2$ vs $\cos^2\phi$ for the tin-antimony alloys.

because of the conditions governing reproducibility from sample to sample have not yet been clearly determined.

2. The Alloys

Examples of the de Haas-van Alphen effect in the 0.026 atomic percent Sb alloy are shown in Figs. 2 and 3. Qualitatively, the features of the effect are similar to those for pure Sn. The phenomenon of beats becomes less noticeable as the Sb concentration is increased and

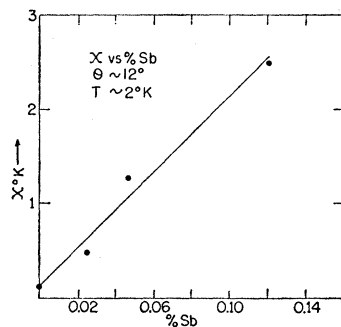


FIG. 5. Plot of X vs atomic percent Sb at $T \approx 2^\circ\text{K}$ and $\phi \approx 12^\circ$.

is practically nonexistent at concentrations of 0.12 atomic percent Sb. The most obvious qualitative effect of increasing the Sb concentration is the decrease in the amplitude of the oscillations.

The significant electronic parameters which occur in Eq. (1) are listed in Table III. These were obtained by fitting the data to Eq. (1) by methods described elsewhere.¹³

Part of the motivation for the present work was to

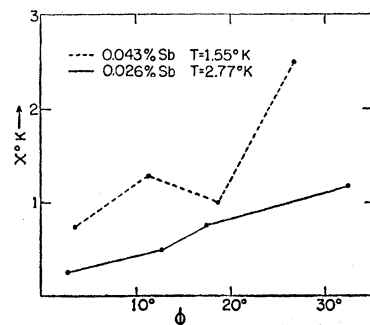


FIG. 6. Plot of X vs ϕ for two tin-antimony alloys.

determine the effect of increasing the electron concentration on the parameter ζ in an effort to decide whether hole or electron motion is responsible for the de Haas-van Alphen effect in Sn. Inspection of Table III shows that within the limits of experimental error (± 10 percent) there is no change in ζ . It appears that the question of holes *versus* electrons as the relevant carriers for the de Haas-van Alphen effect in Sn cannot be decided easily by this method. However, there is evidence that this method is applicable to Bi.¹⁴

The effect of alloying on the period of the oscillations, is shown in Fig. 4, showing a plot of $(2\beta/\zeta)^2$ vs $\cos^2\phi$. There is no detectable change in $2\beta/\zeta$ as the

TABLE III. Tabulation of parameters characterizing the de Haas-van Alphen effect in tin-antimony alloys.

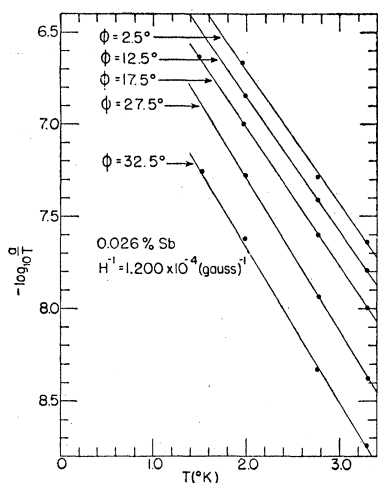
ϕ (deg)	$(2\beta/\zeta) \times 10^7$ (gauss ⁻¹)	Sn X (°K)	ζ (ev)	$2\beta \times 10^{20}$ (ergs/gauss)
1.5	6.21		0.189	18.8
13.5	6.11	0.11	0.198	19.4
16.5	5.89		0.193	18.2
28.5	5.37		0.189	16.2
31.5	5.06	0.10	0.196	15.9
43.5	4.54			
Average = 0.193 ev				
Sn + 0.026% Sb				
2.5	6.77	0.26	0.186	19.6
12.5	6.38	0.61	0.192	19.7
17.5	6.27	0.78	0.186	18.7
27.5	6.00	0.69	0.177	17.0
32.5	5.55	1.20	0.186	16.5
Average = 0.185 ev				
Sn + 0.043% Sb				
3.5	6.46	0.73		
11.5	5.99	1.29		
18.5	5.80	1.00		
33.5	5.03	2.45		
2.2	6.13		0.190	18.6
12.8	5.97		0.203	19.4
17.2	5.85		0.201	18.8
Average = 0.198 ev				
Sn + 0.12% Sb				
3	6.34	2.3	0.183	18.5
12	6.24	2.4	0.199	19.9
18	5.86	2.5	0.210	19.7
27	5.89	1.9	0.193	18.1
42	5.10			
Average = 0.196 ev				

antimony content is increased. In view of the constancy of ζ , this shows that β is also not affected within the limits of experimental error by increasing the Sb concentration in Sn. Thus, the effective mass parameters are not affected by alloying.

Another reason prompting the present work was to determine X , the collision broadening parameter, as a function of the Sb content in Sn under conditions of carefully controlled composition and thermal equilibrium state. In Fig. 5, X as determined at $T \approx 2^\circ\text{K}$

¹⁴ D. Shoenberg and M. Z. Uddin, Proc. Roy. Soc. (London) A156, 687 (1936); Proc. D. Shoenberg Roy. Soc. (London) A170, 341 (1939).

FIG. 7. Plot of $-\log_{10}(a/T)$ vs T for Sn+0.026 atomic percent Sb at various angles, ϕ .



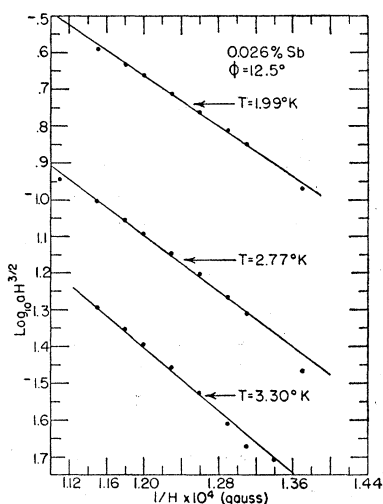
and $\phi \approx 12^\circ$, is plotted as a function of the atomic percentage of Sb added to the Sn. X is an approximately linear function of the Sb concentration and the value for pure Sn is about 0.1°K . This value of X for pure Sn is about ten times smaller than previously quoted values.¹³

In Fig. 6, X vs ϕ is plotted for the 0.026 and 0.043 atomic percent Sb samples. Even though the error in X may be about ± 20 percent, there seems to be a definite dependence of X on ϕ .

In order to compare the theoretical predictions regarding the temperature and field dependence of the amplitude a of the oscillatory part of the susceptibility, $\log_{10}(a/T)$ vs T has been plotted in Fig. 7 and $\log_{10}(aH^{\frac{2}{3}})$ vs H^{-1} in Fig. 8. These data are taken from measurements on the 0.026 atomic percent Sb sample.

If the theoretical predictions are correct, these plots should be straight lines with negative slopes. The temperature dependence of a appears to be accurately predicted, but the field dependence of a shows marked deviations from the predictions. The best average over

FIG. 8. Plot of $\log_{10}(aH^{\frac{2}{3}})$ vs $1/H$ for Sn+0.026 atomic percent Sb at $\phi = 12.5^\circ$ and different T .



the beats, which is indicated, for example, by the dashed lines in Fig. 1, is used to determine a . Further evidence of this deviation from the theoretical predictions is shown for Sn in Fig. 9. Similar results have been observed in Zn.¹⁵

Since X is obtained from the slope of the $\log_{10}(aH^{\frac{2}{3}})$ vs H^{-1} curves, it should be pointed out that the values of X quoted above were obtained by fitting the best straight lines to the curves. In cases where the deviation from linearity was very marked, X was not interpretable and, therefore, not determined.

The room temperature value of $|\chi_3 - \chi_1|$ for the Sn-Sb alloys was also measured and the results are shown in Fig. 10. $|\chi_3 - \chi_1|$ increases linearly by about 25 percent over its value for pure Sn as the percentage of Sb increases by 0.2 atomic percent.

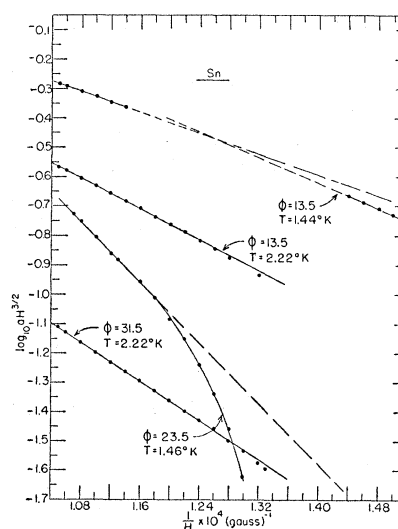


FIG. 9. Plots of $\log_{10}(aH^{\frac{2}{3}})$ vs $1/H$ for pure tin showing strong deviations from linearity.

V. DISCUSSION OF RESULTS

In view of the insensitivity of ζ to increasing electron concentration, the decision between hole conduction or electron conduction as the mechanism responsible for the de Haas-van Alphen effect in Sn cannot be made.

If, for purposes of argument, it is assumed that all the electrons added to Sn as a result of alloying become de Haas-van Alphen effect electrons, there should be a change in ζ given by $\Delta\zeta/\zeta = \frac{2}{3}\Delta N/N$. This amounts to 17 percent at 0.026 atomic percent Sb and 80 percent at 0.12 atomic percent Sb. Since the experimental error in the determination of ζ is ± 10 percent, it follows that less than 0.15×10^{-3} electron per atom become de Haas-van Alphen effect electrons.

The added electrons could become uniformly distributed over the Fermi surface, in which case $(\Delta\zeta/\zeta)$

¹⁵ F. J. Donahoe, and F. C. Nix, preceding paper, Phys. Rev. 95, 1395 (1954).

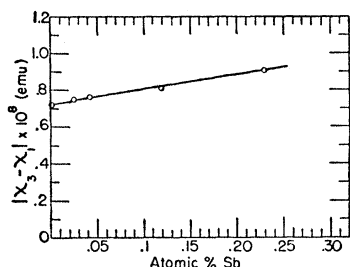


FIG. 10. Variation of $|\chi_3 - \chi_1|$ with atomic percentage of antimony at room temperature.

$\times 100$ would be about 0.2 percent in the 0.12 atomic percent Sb sample, for example, and would not be detectable in the data.

The large change in $\chi_3 - \chi_1$ at room temperature with a very small increase of Sb in the Sn indicates that the added electrons go into a more or less localized region in k space, removed from the regions responsible for the de Haas-van Alphen effect, rather than distribute themselves uniformly over the entire Fermi surface.

A tentative explanation of the variation of X with ϕ is as follows: The parameter X is a function of the reciprocal of the mean free time between collisions for the de Haas-van Alphen electrons. This is demonstrated by Fig. 5, which shows that as the number of Sb atoms in Sn increases, thereby increasing the number of scattering centers, X increases. Since theoretical con-

siderations show that the electron motion in the plane perpendicular to the field is responsible for the de Haas-van Alphen effect, it therefore seems plausible that as the angle between the field and the tetragonal axis of the sample is increased, the plane of the orbits of the de Haas-van Alphen electrons rotates into a more densely packed plane of atoms, which gives rise to shorter mean free times, therefore larger values of X . It is interesting that the value of X at $\phi \cong 30^\circ$ is about three or four times the value of X between 0° and 20° . The de Haas-van Alphen electrons would be rotating in the (101) plane at $\phi = 28.5^\circ$. This plane is more densely packed than the 100 plane in Sn.

The small value of X for pure tin is attributed to the fact that great care was taken to avoid straining the crystal in any way and to the heat treatment given the sample.

At first sight, one might think that the nonlinearity of the $\log_{10}(aH^3)$ vs H^{-1} plots is due to failure to include sufficient terms of the series given in Eq. (3). A calculation of the contribution of the second term, at a reasonable field strength and temperature, to the amplitude shows that it is too small to account for the observed deviations.

It appears that a higher power of H than $3/2$ would give a better fit to the experimental results.

Neutron Diffraction Studies of a Nickel Zinc Ferrite*

V. C. WILSON AND J. S. KASPER

General Electric Research Laboratory, Schenectady, New York

(Received June 8, 1954)

Neutron diffraction studies have been made of a ferrite powder of composition $Zn_{0.5}Ni_{0.5}Fe_2O_4$. The crystal structure is of the spinel type with 4 Zn^{++} and 4 Fe^{+++} ions in the tetrahedral positions and 4 Ni^{++} and 12 Fe^{+++} ions in the octahedral positions. The magnetic structure at $25^\circ C$ appears to have an antiparallel arrangement of the Fe^{+++} spins on the two sites and a random orientation of the Ni^{++} spins.

INTRODUCTION

RECENT neutron diffraction studies of ferrites¹⁻⁴ have clearly demonstrated the special advantages of neutron diffraction for determining both the chemical and magnetic structures of these substances. Thus, while with x-rays it is difficult to ascertain the distribution of the respective cations and even more difficult to obtain a precise value of the oxygen parameter, the use of neutrons readily provides both kinds of information. Even more important is the opportunity by

means of neutron diffraction to obtain directly the location and magnitude of atomic magnetic moments. In the case of $ZnFe_2O_4$ and $NiFe_2O_4$ ² the findings are in agreement with prior postulates as to both the distribution of the ions and the magnetic structures.^{5,6} Thus, $ZnFe_2O_4$ is of the normal spinel type with no magnetic moment alignment, and $NiFe_2O_4$ is of the inverted type with the ferrimagnetic structure proposed by Néel.⁶ It is of interest to ascertain whether the same postulates apply to a ferrite containing both Zn and Ni. The present study was made for this purpose with a specimen of composition $Ni_{0.5}Zn_{0.5}Fe_2O_4$.

* The observations were made at the Brookhaven National Laboratory.

¹ Shull, Wollan, and Koehler, Phys. Rev. **84**, 912 (1951).

² J. M. Hastings and L. M. Corliss, Revs. Modern Phys. **25**, 114 (1953).

³ Corliss, Hastings, and Brockman, Phys. Rev. **90**, 1013 (1953).

⁴ G. E. Bacon and F. F. Roberts, Acta Cryst. **6**, 57 (1953).

⁵ E. J. W. Verwey and E. L. Heilmann, J. Chem. Phys. **15**, 174 (1947).

⁶ L. Néel, Ann. Physik **3**, 137 (1948).